Peer-reviewed version available at *Infrastructures* **2020**, *5*, 70; doi:10.3390/infrastructures5090070

Article

Microstructure Analysis and Strength Characterization of Recycled Base and Subbase Materials using Scanning Electron Microscope

Tanvir Imtiaz [1], Asif Ahmed [2,‡], MD Sahadat Hossain [3,‡] and Mohammad Faysal [4,‡]

[1] Graduate Research Assistant, Dept. of Civil Engineering, The University of Texas at Arlington, 416 S Yates St., Arlington, TX 76019; tanvir.imtiaz@mavs.uta.edu
[2] Assistant Professor, College of Engineering, State University of New York Polytechnic Institute, Utica, NY 13502; asif.ahmed@sunypoly.edu
[3] Professor, Dept. of Civil Engineering, The University of Texas at Arlington, 416 S Yates St., Arlington, TX 76019; hossain@uta.edu
[4] Staff Geotechnical Engineer, D&S Engineering Labs, LLC; Md.faysal@mavs.uta.edu
‡ These authors contributed equally to this work.

Abstract: The reuse of recycled crushed concrete aggregate (RCCA) and reclaimed asphalt pavement (RAP) can provide a sustainable solution for the disposal of C&D materials instead of sending it to landfill. More importantly, it will save energy and reduce impact on the environment. Several states in USA are using RCCA and RAP as base materials for years, focusing on the quality of the recycled materials. The structure of Recycled Aggregate (RA) is more complex than Natural Aggregate (NA). RAs have old mortar adhered on them that forms a porous surface at interfacial transition Zone (ITZ) and prevents new cement mix from bonding strongly with the aggregates. The objective of this work was to correlate microstructural properties like micro-porosity, inter and intra aggregate pores with the unconfined compressive strength (UCS) of RAP and RCCA molds, mixed at different proportions. In this paper, the quantity of micro-pores and their effect on the strength of mixed materials is used as the basis of microstructural analysis of recycled concrete and reclaimed asphalt. Microstructural properties obtained from the analysis of scanning electron microscope (SEM) images were correlated with unconfined compressive strength. Intra-aggregate and inter-aggregate pores were studied for different ratios of cement treated mixture of RAP and RCCA. The results show that the number of pores in the mixture increases considerably by adding RAP, which eventually causes reduction in unconfined compressive strength. In addition, significant morphological and textural changes of recycled aggregates were observed by SEM image analysis.

Keywords: recycled crushed concrete aggregate, reclaimed asphalt pavement, unconfined compressive strength, Microstructure, scanning electron microscope, image analysis)

1. Introduction

Every year approximately 2.6 million tons of recycled crushed concrete aggregate (RCCA) and 100 million tons of reclaimed asphalt pavement (RAP) are generated in US [1]. Instead of disposing of to the landfill, these material can be used as a replacement for natural aggregates (NA) in pavement construction. Use of recycled aggregates can save energy and provide sustainable solution to Construction and Demolition debris (C&D) disposal problem. Pavement rehabilitation projects generate huge amount of waste which are declined by the landfill. The pavement industry is searching for alternative uses of these materials. As base layer contributes most to the structural capacity of flexible pavement systems, high quality materials are essential. The quality of the base course

materials significantly affects the rate of load distribution [2]. Recycled materials have been reported to be a very effective solution for reducing pavement maintenance and construction costs [3]. However, compared to the natural aggregates (NA), recycled aggregates (RA) are weaker [4]. That's why, when recycled aggregates are used as substitute of natural ones for construction of the pavement base, in most cases the minimum requirement of strength standards designated by AASHTO and local state guidelines are not fulfilled [5]. Hence, to comply with the minimum strength requirements different chemical and mechanical stabilization techniques are implemented [6]. Researchers performed a significant amount of investigation to improve the quality of recycled aggregate mixes [7–9].

In 1990s mechanical properties of RAP have investigated by several researchers. [10]. Whereas, very limited numbers of studies have been conducted on the microstructure and its effects on the mechanical properties of recycled concrete aggregate [11]. Recycled aggregates have microstructural features similar to natural aggregates, though it is considerably complex [12]. The contrast is attributed to the diversity inherent to the primary material composition, and strongly dependent on processing and treatment [13]. It also depends on aggregate type and properties [14]. As RAs are broken up progressively, cement paste accumulates in the fine fraction and the density of fine RAs is lower than that of coarse recycled aggregates of the same origin. In addition, recycled aggregates are rougher, more irregular and more angular [13]. As recycled aggregates have more irregular shapes due to their recycling processes, their specific surface areas tend to be higher than those of the natural ones [15,16]. Higher specific surface area is subjected to construct more bonding with cement paste as well as water absorption. This irregular and rough surface area is also responsible for more micro-void in between the bonds.

Microstructural characterisation of recycled aggregate concrete is a powerful tool for determining the above mentioned factors. Cement treated recycled aggregates contain much complex microstructure than concrete with natural aggregates. Microscopic level investigation contribute to the development of the durability and mechanical properties of the complex and heterogeneous material [17]. High microstructural complexity is found due to the heterogeneity of hydrated cementitious products. Strength and durability of the cement treated base can be affected by the porosity of cement paste and the quality of aggregates. These materials have higher porosity than their natural counterparts and are deleterious to the formation of interfacial transition zone (ITZ) with new paste [17]. In cementitious materials a water cement ratio gradient evolves around the aggregates during casting. As a result different microstructure is developed surrounding the hydrated cement paste. This area surrounding the aggregate particles is known as the interfacial transition zone (ITZ) [18]. Porous ITZs weakens the bonding between the cement paste and aggregates. In the normal strength concrete, porous interfacial transition zone microstructure can be ascribed to the higher porosity and absorption capacity of the recycled aggregate [19].

Texas Department of Transportation (TxDOT) guidelines requires minimum compressive strength of 2.068 MPa (300 psi) for base layer of the pavement. Researchers showed that RCCA mixed with up to 50% RAP can be used but must be treated with 4% to 6% cement to meet the minimum requirement [20]. Performance of cement treated recycled aggregates largely depends on the quality and origin of the recycle aggregates used [17]. Inadequate studies on microstructural analysis of cement treated recycled aggregates drives the momentum for this experimental study. Since recycled materials consists of much more porous materials, investigation of their porosity seems decisive. Porosity is related to the compressive strength of a material. Porosity can be different depending upon the distinct mixing ration of RAP and RCCA. However, these mixtures are treated with cement that leads to the change in their chemical composition. Change in chemical and elemental properties can be another function of various strength parameters. Scanning Electron Microscopy (SEM) and Energy Dispersive X-ray Spectroscopy (EDS) were performed on small samples incised from UCS samples, which were prepared at optimum

moisture content with different ratios of RAP and RCCA treated with 6% cement. SEM images were subjected to micro-pore analysis to measure the pore percentage. Furthermore, element percentages found from the EDS were used for the characterization of the strength properties of recycled base materials treated by cement.

2. Materials and Methods

The test program was developed to determine the micro structural properties of the cement treated recycled pavement materials such as reclaimed asphalt pavement and recycled crushed concrete aggregate. To achieve the actual picture of the microstructure of these mixtures without disturbing them, a precise methodology had to be carried out. For the experiment five different mixing ratios of RAP and RCCA, treated with 6% cement were taken into consideration. Scanning electron microscopy and energy dispersive x-ray spectroscopy were performed on those samples. Then the results obtained from these tests were compared to the unconfined compressive strengths of the respective mixtures. Reclaimed asphalt pavement (RAP) and recycled crushed concrete aggregates (RCCA) were collected from the TxDOT specified stockpiles of Big City Crushed Concrete, which is located at Goodnight Lane, Dallas, Texas. Portland Type II cement was used as the binder which has a compressive strength of greater than 50 MPa (7252 psi) at 28 days. Low viscosity epoxy resin and fine sand papers were used to prepare the samples.

2.1. Unconfined Compressive Strength Sample Preparation

Five different combinations of RAP and RCCA were selected for unconfined compressive strength test. The cement content of typical pavements with cement treated base remains within 3% to 10% of the total dry weight of the mixture. In previous studies, 100% RCCA material met the minimum strength criteria of 2.068 MPa (300 psi) at 4% cement content. A combination of 50% RAP and 50% RCCA materials reached the unconfined compressive strength of 2.068 MPa at 5% to 6% cement content. A combination of 70% RAP and 30% RCCA materials fulfilled the minimum strength requirement of 2.068 MPa at 6% cement content [20]. Based on the results from previous studies, each of the combinations were treated with 6% cement. Table 1 represents the material combinations accounted for this experiment.

Table 1. Combinations for experimental program

Mixture Identification		**M1**	**M2**	**M3**	**M4**	**M5**
		0-100-6	10-90-6	30-70-6	50-50-6	100-0-6
Combination	**RAP**	0	10	30	50	100
	RCCA	100	90	70	50	0
	Cement	6	6	6	6	6

For cement treated flex base material unconfined compressive strength (UCS) is one of the important parameters in pavement design. UCS test results serve as the variations of strength and stiffness of the base material with the change of mixing ratio. As labeled from M1 to M5 (Table 1), three samples were prepared for every combination containing 6% cement. All specimen are prepared according to Tex-113-E guidelines [21]. Samples are compacted in a 152.4 mm (6 inch) in diameter and 203.2 mm (8 inch) in height mold at optimum moisture content. As per TxDOT specification a mechanical compactor is used to achieve required compaction. Each specimen are assembled at 4 lifts with 50 blows for each. Specimens are preserved in a moisture room for 7 days at 70 degrees Fahrenheit according to soil-cement testing procedure [22] by TxDOT before testing. Samples are subjected to compressive load using the Universal Testing Machine (UTM) at strain rate of $2.0 \pm 0.3\%$. Following the test procedure of Tex-113E standard method the ultimate load capacity of the sample is taken when it fails at the maximum compressive load.

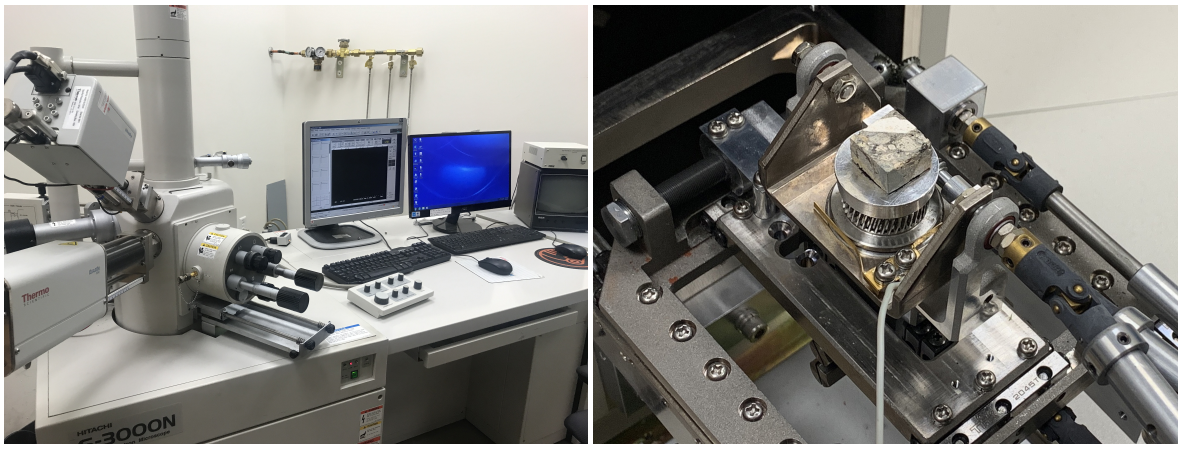

(a) Hitachi 3000N SEM Microscope **(b)** Sample inside SEM Microscope

Figure 1. Scanning electron microscope and sample mount for microscopic observation

2.2. Scanning Election Microscopy

The scanning electron microscope technique is one of the established methods to investigate the surface structure of materials. SEM produces images by probing the sample with a focused beam of electrons, which interact with atoms in the surface to produces various signals that contain information about the material [23]. SEM equipment are coupled to a chemical analysis apparatus such as energy dispersive X-ray spectroscopy (EDS). This apparatus can detect the characteristic of X-rays which is produced by interaction of electrons with the sample material [24]. For our experimental study, Hitachi 3000N SEM Microscope is used to perform both SEM and EDS. Hitachi 3000N SEM Microscope is operated to examine cubed samples at low vacuum (VP-SEM) (Figure 1a). Back-scattered electron imaging (BSE) is performed to detect with a low acceleration voltage ranges from 15 kV to 25 kV. Sample cubes are mounted on a 15mm metal disk using carbon tape.

For micro-pore analysis, 100x magnification is utilized, rather to examine micro-structure 2500x to 3000x magnifications are adopted. Hitachi 3000N SEM machine is also equipped with energy dispersive x-ray spectroscopy that allows to acquire element properties from the same SEM image. From each combination cubes are incised randomly. Images are acquired from four different sides of each cube for the validation of the examination.

2.3. Sample Preparation for Microscopic Observation

SEM samples are collected from the tested UCS samples after 7 days of curing. Pieces of those samples are impregnated in low viscosity epoxy resin [25]. Hardened samples are cut into slices of about 12.7 mm (0.5 inch) thick using diamond blade saw. (Figure 2a). Precautions had been implemented to maintain the integrity of the samples during incision. Incised specimen are polished using SiC sandpaper to ensure smooth surface.

2.4. Image Analysis

To measure the micro-pores in between the aggregates after curing, SEM photographs are taken at 500μm fraction. The captured photographs are used for further analysis. Detectable pores can be identified from the gray-scale contrast. Since the images are black and white, in terms of gray-scale the darkest area of the images can be recognized as porous area. For quantitative analysis of SEM images, vectorization software comes out a handful option[26]. In our study, the images were converted to binary images using the software *imageJ*. Calculating the black and white area, the amount of pores can be measured. At the image, each 1000 pixels were considered equal to 1mm [17]. Average

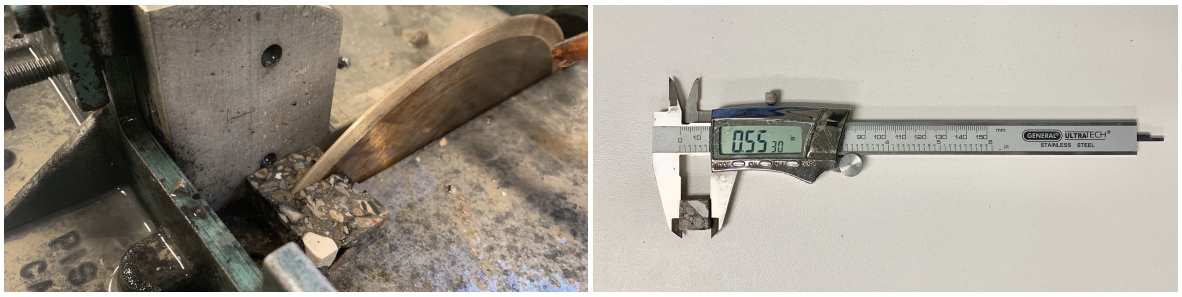

(a) Diamond blade saw **(b)** Sample measurement

Figure 2. Scanning electron microscope sample preparation for microscopic observation

value from all measured pore area for each combination was taken as the amount of pores for that combination.

3. Results and Analysis

3.1. Qualitative Analysis

Microstructural study of different heterogeneous material such as RCCA and RAP treated with lower amount of cement illustrates distinctive hydration products. Density, shape, and size; pore structure, stability, and strength are the main properties of the aggregates influencing concrete behavior. [27] Whether in microscopy study of concrete calcium hydroxide (CH), tricalcium disilicate hydrate (C-S-H), pores and residual unhydated cement are the significant components to analyze. Various field image analysis process are developed to analyze the quantity and quality of these properties. [14] C-S-H is mostly responsible for the behavior and strength of the hardened cement. [28] RCCA and cement paste share almost similar chemical behaviour. RCCA consists of significant amount of fine aggregates which are basically the old mortars. Difference between natural aggregate and recycled aggregate can be distinguished by the presence of ettringite (spike like crystal). $3CaO \cdot SiO_2$, $2CaO \cdot SiO_2$ and $3CaO \cdot Al_2O_3$ and the solid solution with average composition $4CaO \cdot Al_2O_3 \cdot Fe_2O_3$ are the fundamental components of cement. [27]. During hydration, $3CaO \cdot Al_2O_3$ reacts with gypsum $CaO \cdot SO_3 \cdot 2H_2O$ to sequentially form the hydrous calcium aluminum sulfate ettringite $Ca_6Al_2(SO_4)_3(OH)_{12} \cdot 26H_2O$ and monosulfate. These are the initial reactions which occur during first 24 hours of hydration. Further reactions produce C-S-H which strengthen the material [28]. Figure 3a illustrates the presence of ettringite and C-S-H. However, RAP usually do not perform hydration reaction due to their asphalt overlay. RAP aggregates are partially to fully covered by bituminous binders that prevents them to react with cement. In figure 3b round crooked shape asphalt overlay is detected incorporated with air voids.

3.2. Pore Analysis

Back-scatter SEM can usually detect a significant amount of visible pore area in most cement treated compositions. Epoxy resin fills the pore spaces in prepared samples. Because of the ability of low electron back-scattering epoxy resin filled pores appear darker than other materials in the composition[29]. So the secondary electron images are converted to 8-bit binary image in gray scale having intensity of 0 (black) and 255 white (white) [30]. In terms of porosity, four features of a pore system are (a) micropores in the 0.5 to 10 nm range (gel pores), (b) mesopores in the 5 to 5,000 nm range (capillary pores), (c) macropores due to compaction and (d) shrinkage cracks are taken into consideration [31]. Except the pores smaller than a pixel, [14] the darker area of the binary images are considered as pores. Area of pores is calculated using the *imageJ* software. SEM photographs are captured on four randomly incised cube for each RAP-RCCA combinations to ensure representativity. The average of the percentages represents the amount of pores found in that combination. The amount

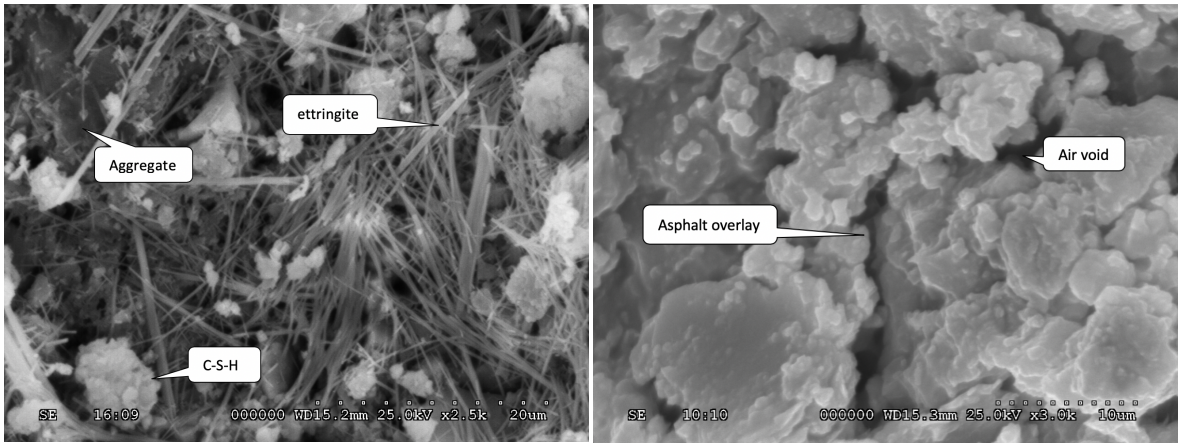

(a) Secondary electron image of RCCA **(b)** Secondary electron image of RAP

Figure 3. Scanning Electron Microscope image of (**a**) RCCA and (**b**) RAP

to average pore percentage increased with the substitution of 0, 10, 30, 50 and 100 percent RAP material. Average pore percentages are found 4.85, 5.95, 8.01, 10.49 and 16.49 percent respectively. Table 2 shows average area of pores in each combinations.

Table 2. Area of Pores

Combination ID	Area of Pores (%)	Average Area of Pores
M1	3.767 5.820 7.458 2.345	4.85
M2	3.690 6.580 5.140 8.381	5.95
M3	9.713 7.121 3.907 11.290	8.01
M4	11.387 5.980 15.489 9.088	10.49
M5	9.607 3.437 20.365 32.543	16.49

For instance, Figure 4 and Figure 5 present the binary conversion from scanning electron microscopic image for 30% RAP, 70% RCCA and 100% RAP, 0% RCCA stabilized with 6% cement respectively. The larger pores correspond to entrapped air bubbles due to the inadequate compaction. In RCCA these pores are gradually filled by hydration reaction with residual cementitious material and newly formed CH [19,27]. Whether asphalt overlay restricts the RAP aggregates to react thus unable to fill the pores.

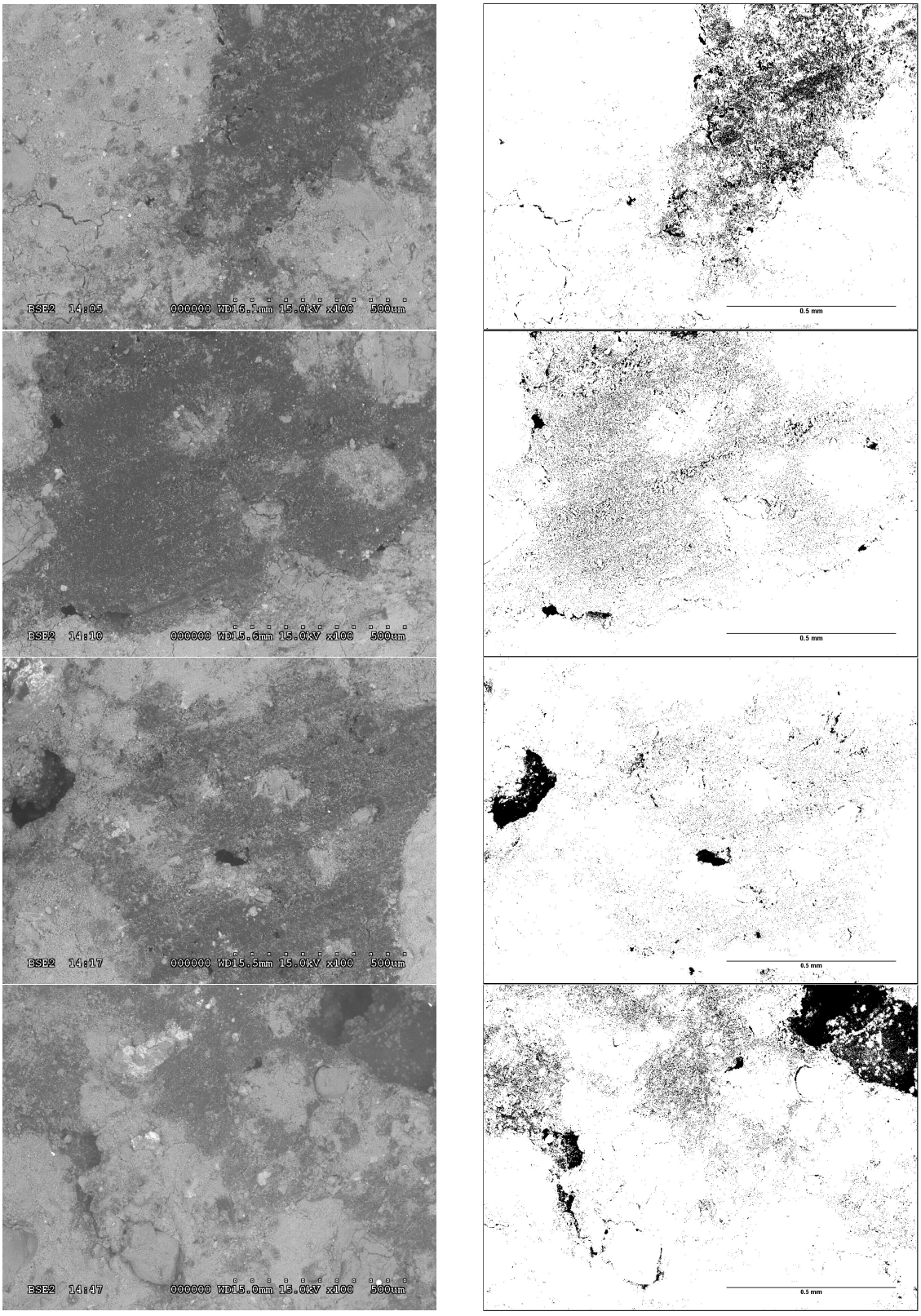

Figure 4. SEM (left) and binary image (right) of 30% RAP, 70% RCCA with 6% cement

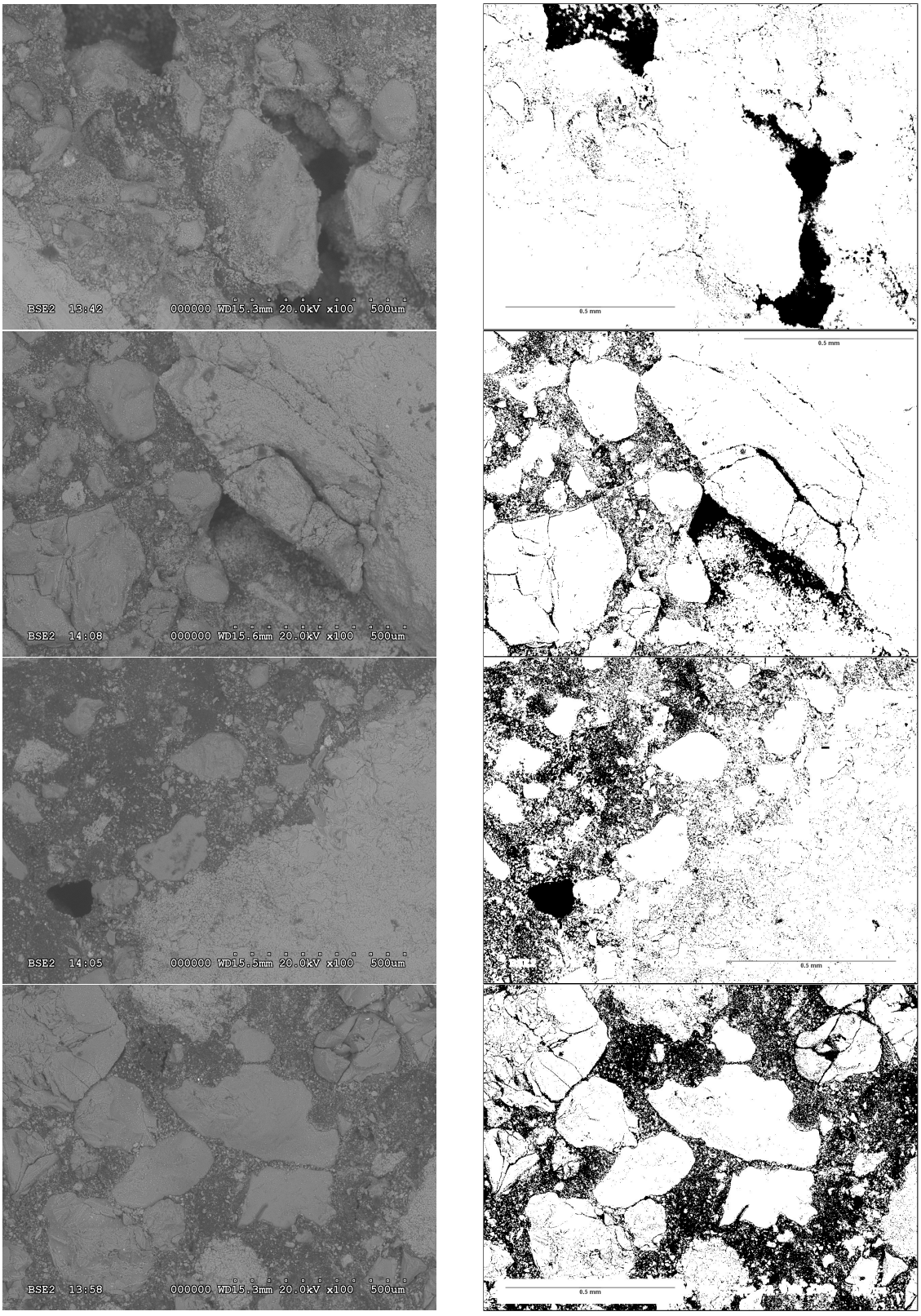

Figure 5. SEM (left) and binary image (right) of 100% RAP, 0% RCCA with 6% cement

3.3. Porosity and Compressive Strength

Porosity has a significant impact on the strength of aggregate blend for the treated base. Porous substances are generally weaker than solid objects. Compressive strength is correlated to the porosity of that material.

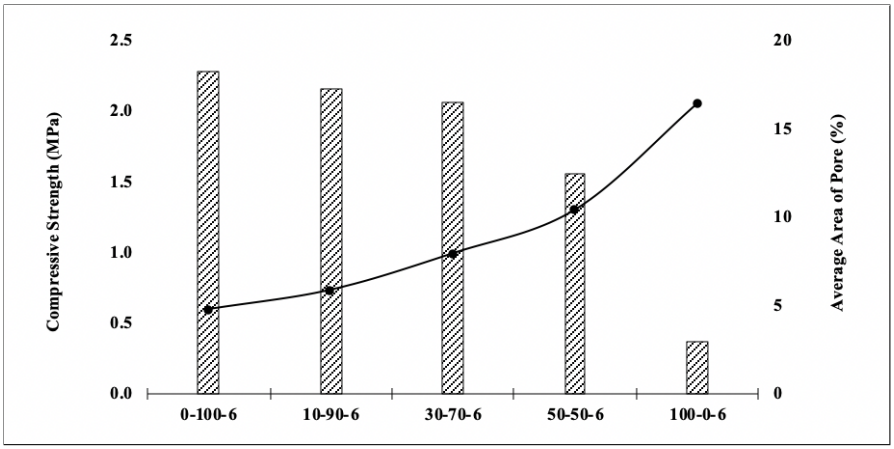

Figure 6. Comparison of unconfined compressive strength with porosity

In Figure 6 compressive strength is represented along with the average percentage of pores for different combinations of RCCA and RAP treated by 6% cement. Compressive strength decreases with the increase of percentage of pores. Due to the growing of hydrated compounds that have hydraulic properties, amount of pores reduces thus the compressive strength increases[32]. Higher percentage of RAP aggregates create more voids than RCCA in aggregate blends. As hydration products tent to migrate into pores, in RCCA pores are being filled up. Interfacial transition zone (ITZ) is often found the weakest part of the concrete [33]. Asphalt overlay makes porous ITZ resulting weaker bonding between them. As of Figure 10a the average area of pore shows an increasing trend with the increase of compressive strength; which is decreasing the intrusion of RAP material.

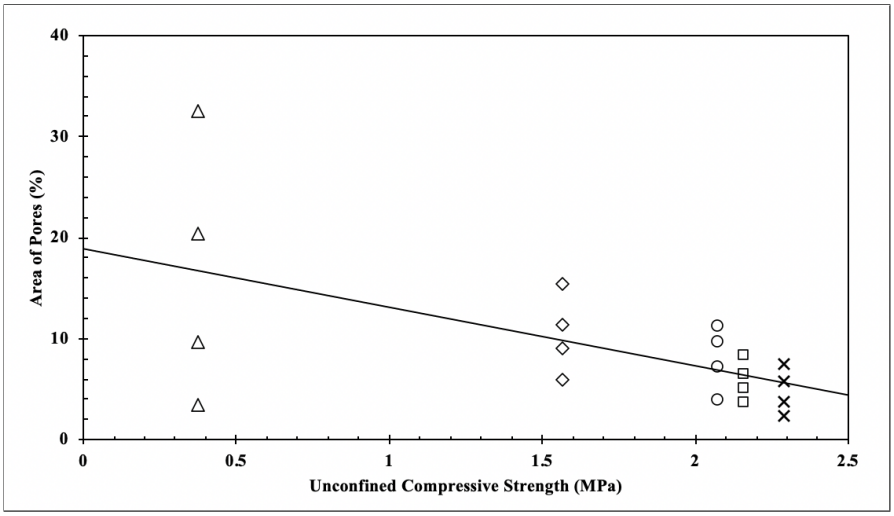

Figure 7. Percentages of pore area against the unconfined compressive strength

3.4. Energy Dispersive Spectroscopy

Energy dispersive x-ray spectroscopy comes with the SEM exhibits the EDS spectrum along with average weight percentage of each element present on that image [3]. In Figure 8(a), 100% RCCA is treated with 6% cement demonstrates highest count of Silicon (Si) on the other hand in Figure 8(b),

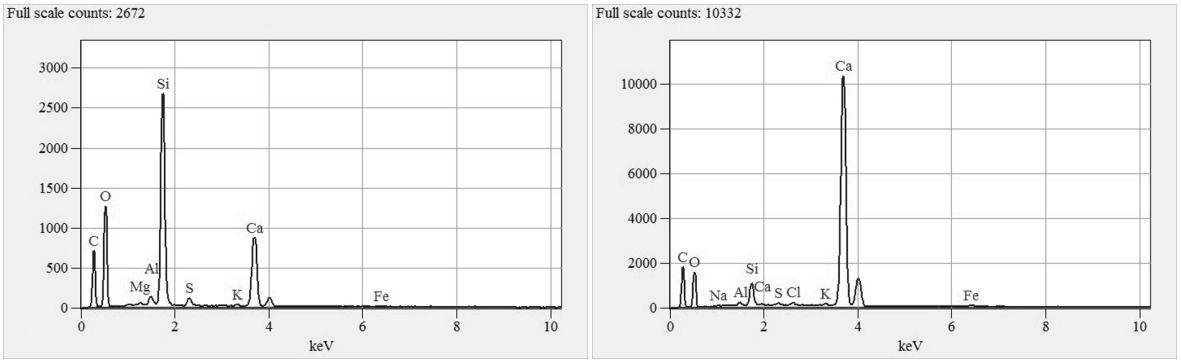

(a) **(b)**

Figure 8. Energy Dispersive X-ray Spectrum of (**a**) 0% RAP + 100% RCCA + 6% cement (**b**) of 100% RAP + 0% RCCA + 6% cement

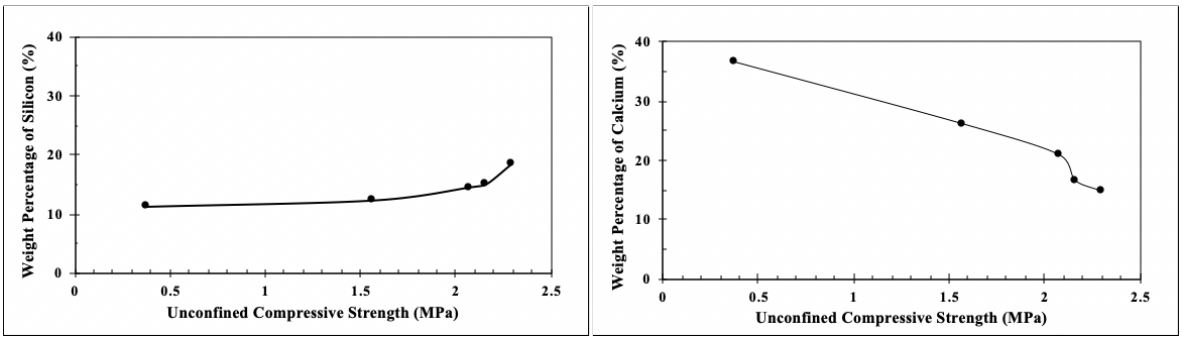

(a) **(b)**

Figure 9. Weight percentage of (**a**) Silicon and (**b**) Calcium with the variation of compressive strength

Calcium (Ca) shows the highest count in the spectrum. However, from the NSS software we can get the average percentage of each element in a tabular form. Compressive strength decreases with the intrusion of RAP material, we observed an increase in Calcium percentage as such 14.79, 16.59, 20.92, 26.17 and 36.68 respectively (Figure 9a) However, Si decreased with the decrease compressive strength as follows 18.33, 14.93, 14.45, 12.23 and 11.16 (Figure 9b).

3.5. Ca/Si Ratio and Compressive Strength

The fundamental element of hydrated cement paste, the carbonation behavior of C-S-H mainly depends on its structure, which is affected by the Ca/Si ratio[34]. Change in C-S-H gel significantly impacts the strength characteristics of hardened cement paste. Researchers found a significant increase in compressive strength for low Ca/Si value of C-S-H paste whereas comparatively less compressive strength at high Ca/Si value [35]. In this experimental study, we observed the similar trend of increasing compressive strength with the increase of Ca/Si ratio. Figure 10b represents the co-relation between compressive strength and Ca/Si ratio with a R^2 value of 0.9647.

4. Discussion

The detection of different sizes of pores are limited by the resolution of SEM images. The minimum size of a pore must be a size of a dark pixel in the image. That means the pores of sizes less than about $0.2\mu m$ are not discoverable at the usual range of magnifications generally . However, as indicated in previous research works much finer pores can be seen in FE-SEM examination[36]. Nevertheless, the lower limit of conventional SEM-detectable pore sizes is usually larger than the upper limit of pore sizes reported in mercury intrusion porosimetry study of hydrated cement paste; the latter is often significantly less than 0.1 μm. Pores detected by SEM images demonstrate that commonly used mercury intrusion method underestimates the smaller pores which are actually present in the

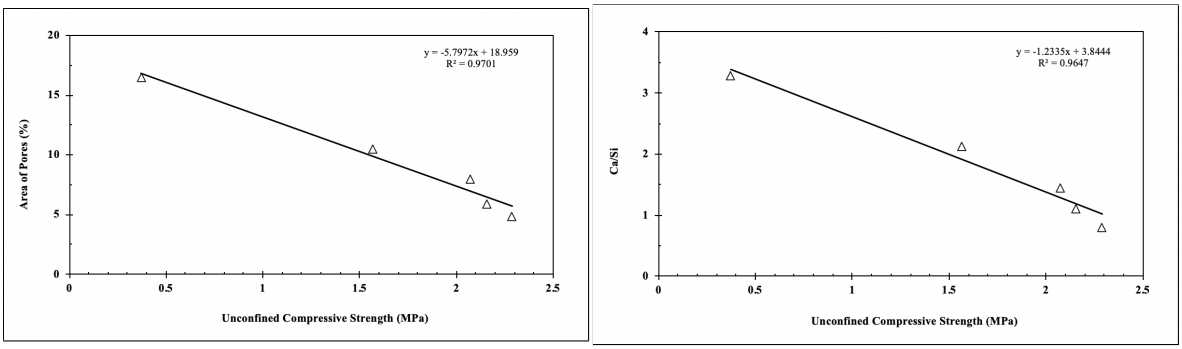

(a) **(b)**

Figure 10. Variation of compressive strength with (**a**) area of pores and (**b**) Ca/Si ratio

image[29]. Our method of calculating average area of pores are based on a very few test samples. However, these primary analysis indicates that quality of recycled aggregates can be utilized. More SEM-EDS data of different RAP-RCCA combinations at various cement content might establish the co-relation of pore area and Ca/Si ratio with unconfined compressive strength.

5. Conclusion

Based on our experimental study, characterization of such heterogeneous material such as recycled aggregates, microstructural analysis might be accepted as a convenient approach. This experimental study on the microstructural and elementary properties of different combinations of recycled aggregate blends concludes some far-reaching features that can be beneficial for further research.

- Microscopic photographs can distinguish between recycled aggregate and natural aggregates. Recycled aggregates are weaker than natural aggregates. Microstructure of recycled aggregates are heterogeneous, irregular and inconsistent. Recycled crushed concrete is progressively broken up and mostly covered by old cement mortar and fine fractions.
- Recycled asphalt aggregates are mostly covered by asphalt layer that prevents formation of new cement-aggregate bonding, as such replacing greater portion of RAP in aggregate blends significantly reduces the compressive strength and stiffness.
- Porosity of hundred percent RAP blend material is around 3 times than the Porosity of hundred percent RCCA blend material. Porosity increases gradually with the increase of RAP as a replacement of RCCA.
- Compressive strength decreases linearly as the area of pores decreases. Compressive strength increase with the increase of weight percentage of silicon whether the strength decreases with the increase calcium percentage.
- Compressive strength is higher at low Ca/Si ratio but lower at high Ca/Si value. Strength increases linearly with the Ca/Si ratio.

Author Contributions: In this research project authors have the following individual contributions: conceptualization, Tanvir Immtiaz, Asif Ahmed, MD Sahadat Hossain and Mohammad Faysal; investigation, methodology, software, Tanvir Imtiaz; validation, formal analysis, Tanvir Imtiaz and Asif Ahmed; resources, MD Sahadat Hossain; writing–original draft preparation, Tanvir Imtiaz, Asif Ahmed, MD Sahadat Hossain and Mohammad Faysal; writing–review and editing, Tanvir Imtiaz, Asif Ahmed, MD Sahadat Hossain and Mohammad Faysal; supervision, project administration, MD Sahadat Hossain.

Funding: This research was funded by TxDOT Dallas District

Acknowledgments:

Conflicts of Interest: The authors declare no conflict of interest. The funders had no role in the design of the study; in the collection, analyses, or interpretation of data; in the writing of the manuscript, or in the decision to publish the results.

Abbreviations

The following abbreviations are used in this manuscript:

C&D	Construction and Demolition debris
EDS	Energy Dispersive X-ray Spectroscopy
ITZ	Interfacial Transition Zone
NA	Natural Aggregate
RA	Recycle Aggregate
RAP	Reclaimed Asphalt Pavement
RCCA	Recycled Crushed Concrete Aggregate
SEM	Scanning Electron Microscope
UCS	Unconfined Compressive Strength

References

1. Copeland, A. Reclaimed asphalt pavement in asphalt mixtures: State of the practice. Technical report, TRID, 2011.
2. Potturi, A. Evaluation of resilient modulus of cement and cement-fiber treated reclaimed asphalt pavement (RAP) aggregates. *Journal of Materials in Civil Engineering* **2007**.
3. Ordonez, C.A. Characterization of cemented and fiber-reinforced RAP aggregate materials for base/sub-base applications. *Journal of Materials in Civil Engineering* **2007**.
4. Taha, R.; Ali, G.; Basma, A.; Al-Turk, O. Evaluation of reclaimed asphalt pavement aggregate in road bases and subbases. *Transportation Research Record* **1999**, *1652*, 264–269.
5. Rana, A. Evaluation of recycled material performance in highway applications and optimization of their use. PhD thesis, Texas Tech University, 2004.
6. Sobhan, K.; Mashnad, M. Mechanical stabilization of cemented soil–fly ash mixtures with recycled plastic strips. *Journal of environmental engineering* **2003**, *129*, 943–947.
7. Taha, R.; Al-Harthy, A.; Al-Shamsi, K.; Al-Zubeidi, M. Cement stabilization of reclaimed asphalt pavement aggregate for road bases and subbases. *Journal of materials in civil engineering* **2002**, *14*, 239–245.
8. Guthrie, W.S.; Cooley, D.; Eggett, D.L. Effects of reclaimed asphalt pavement on mechanical properties of base materials. *Transportation Research Record* **2007**, *2005*, 44–52.
9. Grilli, A.; Bocci, E.; Graziani, A. Influence of reclaimed asphalt content on the mechanical behaviour of cement-treated mixtures. *Road Materials and Pavement Design* **2013**, *14*, 666–678.
10. Kolias, S. Mechanical properties of cement-treated mixtures of milled bituminous concrete and crushed aggregates. *Materials and Structures* **1996**, *29*, 411–417.
11. Sagoe-Crentsil, K.K.; Brown, T.; Taylor, A.H. Performance of concrete made with commercially produced coarse recycled concrete aggregate. *Cement and concrete research* **2001**, *31*, 707–712.
12. Akhtar, A.; Sarmah, A.K. Construction and demolition waste generation and properties of recycled aggregate concrete: A global perspective. *Journal of Cleaner Production* **2018**, *186*, 262–281.
13. Silva, R.V.; De Brito, J.; Dhir, R.K. Properties and composition of recycled aggregates from construction and demolition waste suitable for concrete production. *Construction and Building Materials* **2014**, *65*, 201–217. doi:10.1016/j.conbuildmat.2014.04.117.
14. Diamond, S. Considerations in image analysis as applied to investigations of the ITZ in concrete. *Cement and Concrete Composites* **2001**, *23*, 171–178. doi:10.1016/S0958-9465(00)00085-8.
15. Solyman, M. Classification of Recycled Sands and their Applications as Fine Aggregates for Concrete and Bituminous Mixtures. *Klassifizierung von Recycling -Brechsanden und ihre Anwendungen für Beton und für Straßenbaustoffe* **2005**, p. 170.
16. Evangelista, L.; Guedes, M.; De Brito, J.; Ferro, A.C.; Pereira, M. Physical, chemical and mineralogical properties of fine recycled aggregates made from concrete waste. *Construction and building materials* **2015**, *86*, 178–188.
17. Evangelista, L.; Guedes, M. Microstructural studies on recycled aggregate concrete. *New Trends in Eco-efficient and Recycled Concrete* **2018**, *24*, 425–451. doi:10.1016/b978-0-08-102480-5.00014-2.
18. Ollivier, J.P.; Maso, J.C.; Bourdette, B. Interfacial transition zone in concrete. *Advanced Cement Based Materials* **1995**, *2*, 30–38. doi:10.1016/1065-7355(95)90037-3.

19. Poon, C.; Shui, Z.; Lam, L. Effect of microstructure of ITZ on compressive strength of concrete prepared with recycled aggregates. *Construction and Building Materials* **2004**, *18*, 461–468. doi:10.1016/J.CONBUILDMAT.2004.03.005.
20. Faysal, M. Structural competency and environmental soundness of the recycled base material in north Texas. PhD thesis, University of Texas at Arlington, 2017.
21. TxDOT-113-E. TxDOT-113-E: Laboratory Compaction Characteristics and Moisture-Density Relationship of Base Materials. *TxDOT Research Reports and Products* **2016**, pp. 1–15.
22. TxDOT-120-E. Soil-Cement Testing. *Texas Department of Transporatation* **2013**, pp. 5–9.
23. Microscopy, S.E.; Microanalysis, X.R. JI Goldstein, DE Newbury, P. Echlin, DC Joy, C. Fiori, and E. Lifshin, 1981.
24. Evangelista, L.; Guedes, M. 14 - Microstructural studies on recycled aggregate concrete. In *New Trends in Eco-efficient and Recycled Concrete*; [de Brito], J.; Agrela, F., Eds.; Woodhead Publishing Series in Civil and Structural Engineering, Woodhead Publishing, 2019; pp. 425 – 451. doi:https://doi.org/10.1016/B978-0-08-102480-5.00014-2.
25. Bonifazi, G.; Capobianco, G.; Serranti, S.; Eggimann, M.; Wagner, E.; Di Maio, F.; Lotfi, S. The ITZ in concrete with natural and recycled aggregates: Study of microstructures based on image and SEM analysis. *Proceedings of the 15th Euroseminar on Microscopy Applied to Building Materials* **2015**, pp. 299–308.
26. Tang, Y.q.; Zhou, J.; Hong, J.; Yang, P.; Wang, J.x. Quantitative analysis of the microstructure of Shanghai muddy clay before and after freezing. *Bulletin of Engineering Geology and the Environment* **2012**, *71*, 309–316.
27. Domone, J.; Illston, J. Concrete. *Construction Materials: Their Nature and Behaviour* **1998**, pp. 89–195.
28. Evangelista, L.; Guedes, M.; Ferro, A.; de Brito, J. Microstructure of concrete prepared with construction recycled aggregates. *Microscopy and Microanalysis* **2013**, *19*, 147–148.
29. Diamond, S. The microstructure of cement paste and concrete—-a visual primer. *Cement and Concrete Composites* **2004**, *26*, 919–933.
30. Falchetto, A.C.; Moon, K.H.; Wistuba, M.P. Microstructural analysis of asphalt mixtures containing recycled asphalt materials using digital image processing. *6th Eurasphalt & Eurobitume Congress* **2016**.
31. Kumar, R.; Bhattacharjee, B. Porosity, pore size distribution and in situ strength of concrete. *Cement and concrete research* **2003**, *33*, 155–164.
32. Largo, O.R.; de la Villa, R.V.; de Rojas, M.S.; Frías, M. Novel use of kaolin wastes in blended cements. *Journal of the American Ceramic Society* **2009**, *92*, 2443–2446.
33. van Breugel, K.; Koenders, E.; Guang, Y.; Lura, P. Modelling of transport phenomena at cement matrix—aggregate interfaces. *Interface Science* **2004**, *12*, 423–431.
34. Li, J.; Yu, Q.; Huang, H.; Yin, S. Effects of Ca/Si Ratio, Aluminum and Magnesium on the Carbonation Behavior of Calcium Silicate Hydrate. *Materials* **2019**, *12*, 1268.
35. Kunther, W.; Ferreiro, S.; Skibsted, J. Influence of the Ca/Si ratio on the compressive strength of cementitious calcium–silicate–hydrate binders. *Journal of Materials Chemistry A* **2017**, *5*, 17401–17412.
36. Kjellsen, K.O.; Monsøy, A.; Isachsen, K.; Detwiler, R.J. Preparation of flat-polished specimens for SEM-backscattered electron imaging and X-ray microanalysis - Importance of epoxy impregnation. *Cement and Concrete Research* **2003**, *33*, 611–616. doi:10.1016/S0008-8846(02)01029-3.